

# Decarbonising Electrical Grids using Photovoltaics with Enhanced Capacity Factors Supplemental Information

Cai Williams<sup>a</sup>, Hannes Michaels<sup>b</sup>, Andrew F. Crossland<sup>c</sup>, Zongtai Zhang<sup>a</sup>, Natasha Shirshova<sup>a</sup>, Roderick C. I. MacKenzie<sup>a</sup>, Hongjian Sun<sup>a</sup>, Jeff Kettle<sup>d</sup>, Marina Freitag<sup>b</sup>,  
Christopher Groves<sup>a,\*</sup>

<sup>a</sup>*Department of Engineering, Durham University, South Road, DH1 3LE, UK*

<sup>b</sup>*Department of Chemistry, Bedson Building, Newcastle University, Newcastle upon Tyne, NE1 7RU, UK*

<sup>c</sup>*Durham Energy Institute, Durham University, South Road, DH1 3LE, UK*

<sup>d</sup>*James Watt School of Engineering, University of Glasgow, Glasgow, Scotland, UK*

---

\*chris.groves@durham.ac.uk



generation of both wind and solar from assets present in 2016 are taken from BMRS<sup>2</sup>. For experiments described in the main paper in which additional Solar assets with Silicon or CFPV devices, the additional generation is calculated using the methodology described in section 2 of the SI.

<b>Dispatch Class</b>	<b>Generation Type</b>	<b>Installed Capacity (MW)<sub>2</sub></b>	<b>Carbon Intensity (gCO<sub>2</sub>eq/kWh)<sub>3</sub></b>
1	Nuclear	8,981	12
2	Solar	11,970* <sup>4</sup>	48
2	Wind Onshore	8,562	11
2	Wind Offshore	5,011	12
2	Hydro Run-of-River and Poundage	1,540	24
3	Hydro Pumped Storage	2,744	24
4	Fossil Gas	25,702	490
4	Fossil Hard Coal	14,889	820

Table S1: The Installed capacity and carbon intensity of each generation types. \*Due the balancing mechanism reporting service not counting assets less than 50 MW towards the installed capacity (which artificially reduces the actual installed capacity), the installed capacity reported by PVLive<sup>4</sup> at the end of the year is used.

<b>Dispatch Class</b>	<b>Total Capacity (MW)</b>
1	8,981
2	27,083
3	2,744
4	40,591
Total	82,098

Table S2: Total capacity of each dispatch class and overall total capacity in 2016 sourced from BMR<sup>2</sup>.

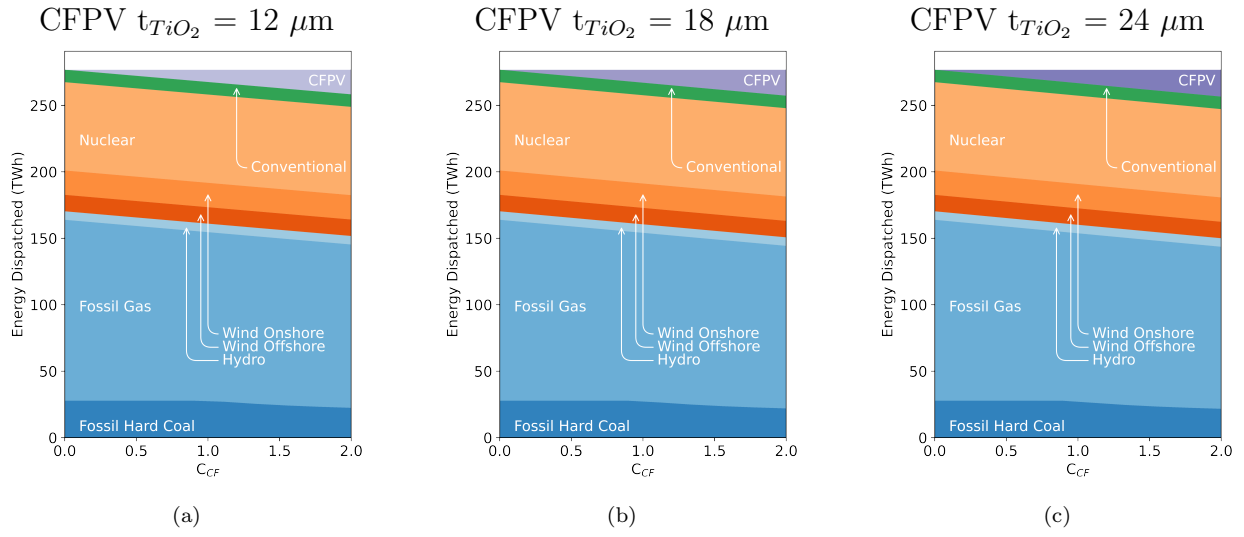


Figure S2: Annual energy dispatched as a function of additional CPFV capacity. Figures (a,b,c) show the source of carbon savings from reduction in Gas (Light Blue) and Coal (Dark Blue) emissions.

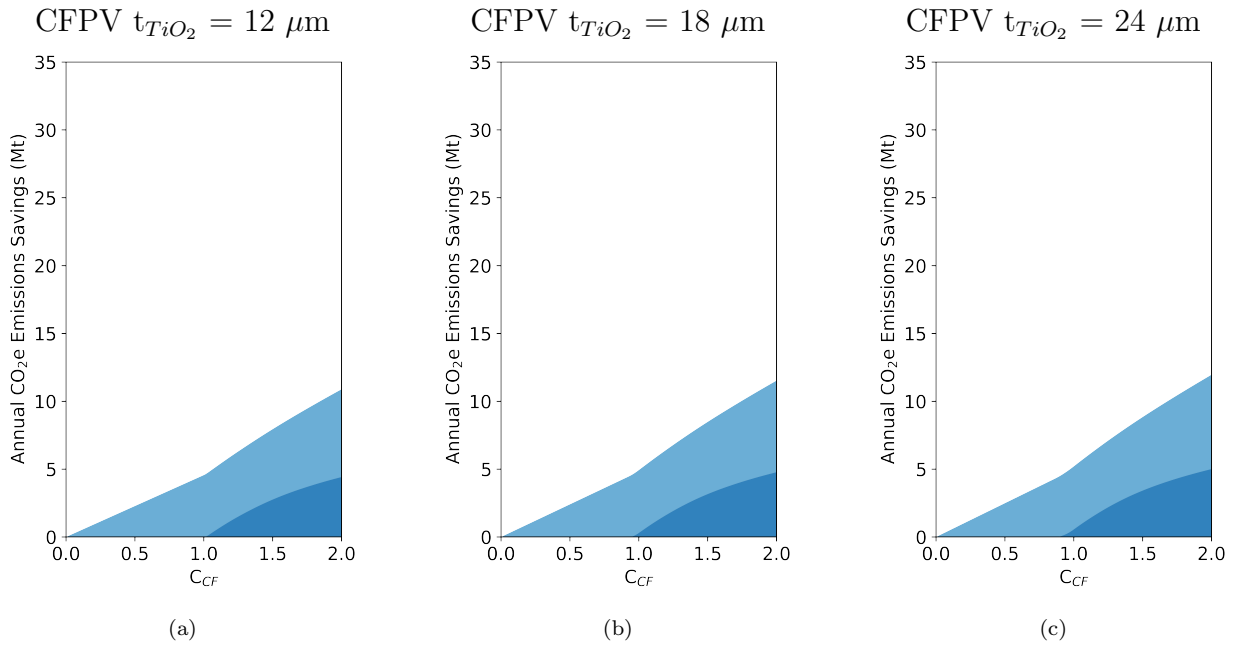


Figure S3: Annual carbon savings as a function of additional CPFV capacity. Figures (a,b,c) show the source of carbon savings from reduction in Gas (Light Blue) and Coal (Dark Blue) emissions.

## 2. Modelling UK Solar PV generation

### 2.1. Calculating generation from additional solar assets

Within the model, additional PV generation,  $G$  (Wh) over and above pre-installed PV capacity in 2016 was calculated in each time window as follows:

$$G(l, t) = \frac{C}{C_{2016}} \times G_{PV}(t) \times E(l) \quad (1)$$

Where  $C$  was the additional installed capacity of either Silicon or CFPV,  $C_{2016}$  was the the generation capacity of PV in the UK in 2016 (11,970 MW, Table S1),  $G_{PV}(t)$  was the aggregated historical PV generation at time  $t$  in 2016 from BMRS<sup>2</sup>, and  $E(l)$  was the enhancement factor at the time interval  $t$  for which the irradiance was  $l$ . Thus, within the model, the generation of CPFV and silicon PV differed by the factor  $E$ , which was defined as:

$$E(l) = \frac{PCE(l)}{PCE(1000)} \quad (2)$$

### 2.2. Determining irradiance dependent enhancement factors

To determine the irradiance dependant scaling factors, two pieces of data were used i) the PCE-irradiance characteristic of the chosen device, describing the performance of the device at various irradiance levels, and ii) historical irradiance data for the same period as the historical generation data used by the dispatch model.

For silicon devices,  $E = 1$ . For CFPV devices, the value of  $E$  for the relevant value of  $l$  within the time period was calculated from experimental data in the following way. For values of irradiance which match those reported by the enhancement-irradiance characteristic the exact experimental enhancement values are used. For values of  $l$  which lay in between experimental datapoints a linear interpolation was applied between the two adjacent reported points to calculate the enhancement, for values which lie outside the range of reported by the characteristics a linear interpolation was made from the nearest two values.

### 2.3. Locations

Referring to equation 1, PV generation is scaled from historical generation for conventional PV by both the additional capacity of solar ( $C$ ) and enhancement factor ( $E$ ). Thus our approach implies that additional PV generation capacity is being added to pre-existing solar farm locations. Each of these locations may have a different instantaneous irradiance  $l$ , and therefore different enhancement factor  $E$ , per equation 2. In the UK, there are estimated to be upwards of 861 solar farms with capacity more than  $5\text{MW}_P$ <sup>4</sup>. Hence we took the following approach to investigate how these differing locations, and therefore range of enhancement factors should be accounted for in the model.

We first used a single location ( $N = 1$ ) to determine the enhancement factor  $E$ . This location had an average annual irradiance for the mainland UK as determined from Global Solar Atlas<sup>5</sup> (Latitude: 53.13359 and Longitude: -1.746826). Figure S4 shows predicted annual generation using the enhancement factor for this single location ( $N = 1$ ) when a capacity of  $C_{CF} = 1$  of the SolarPrint device was installed on the network and no conventional Solar PV. We selected these parameters as they were viewed to be a stress test of the assumptions.

We then ran further simulations in which the same capacity of solar (i.e.  $C_{CF} = 1$  of SolarPrint) was installed, but with enhancement factors drawn from random locations within the mainland UK, and using the average enhancement factor for these locations in equation 1. For clarity, the location with average irradiance described previously was not used. The number of locations was increased from  $N = 2$  to 1000, and the predicted annual energy generation is shown in Fig. S4. It was observed that the predicted energy generation increased by  $\sim 6\%$  when  $N$  increased from 1 (i.e. a single average irradiance location) to 2 (i.e. two random locations), and stayed largely constant thereafter.

The assumption of  $N = 1$  is therefore shown to underestimate the energy generation for CFPV devices by  $\sim 6\%$ , and thus underestimates the efficacy of CFPV devices described in the paper. Notwithstanding this, we opted to use  $N = 1$  for reasons of computational efficiency. The results presented should therefore be viewed as a lower bound of the efficacy of CFPV devices.

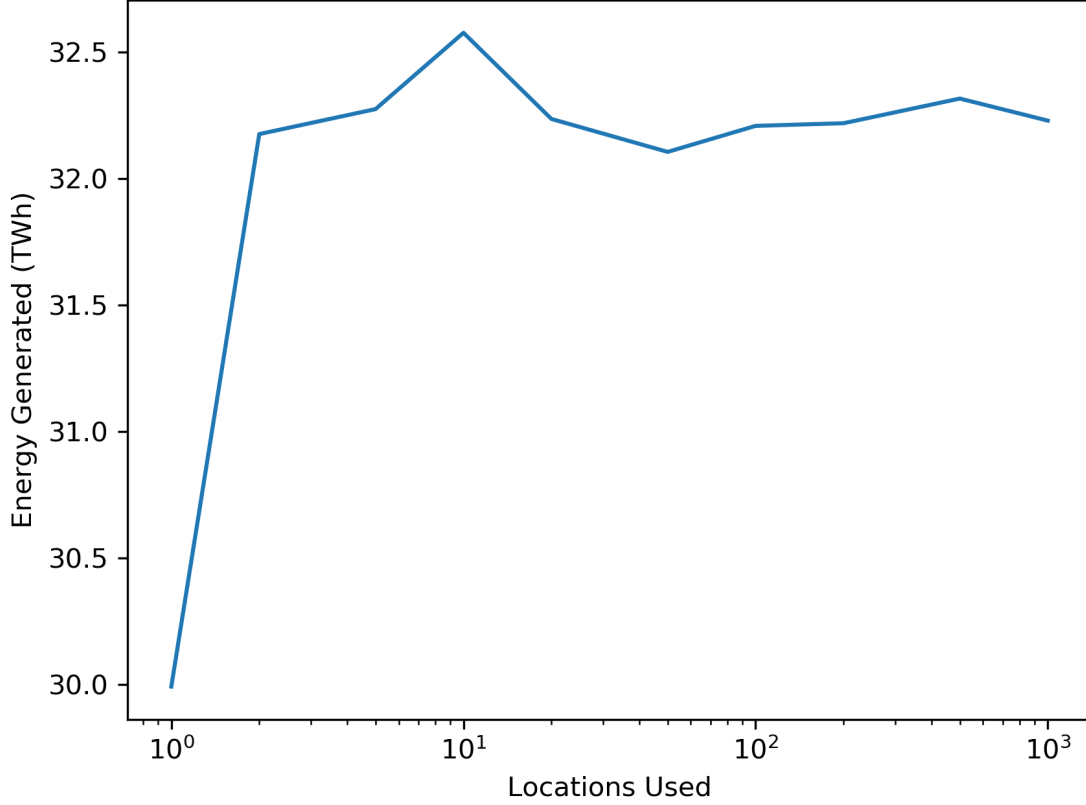


Figure S4: Energy generated by introduced solar assets when varying the number of locations used to calculate enhancement data. Locations when greater than 1 were randomly chosen from the land area of Britain and the average enhancement of said locations is used calculated and applied to the model.

#### 2.4. DC to AC ratio and clipping

It is standard practice for the inverter, which converts the DC power from the solar modules to AC so that it can join the grid, to be rated at a lower capacity than the solar panels connected to it. This DC/AC ratio ( $>1$ ) will be selected based on the predicted energy yield in the chosen location as well as the costs of solar panels and inverters. DC/AC ratios in the range 1.1 to 1.3, are common in the UK. Practically the DC/AC ratio may limit the power output from a solar farm (by 'clipping') during periods of high irradiance, i.e. when:

$$DC/AC_{ratio} < \frac{1000}{l} \quad (3)$$

We would expect that CPFV devices would change the optimal DC/AC ratio as compared to conventional Si PV devices. However, we view this detail to be out scope from the current paper since the impacts of clipping are expected to be small (e.g. Fig. 3 in the main text). Further we stress that the optimal DC/AC ratio would be specific to the location of the solar farm, and as such, is at a more granular level of detail than the national analysis presented here. Future work will investigate the benefits of CFPV to the wider electrical network, as well as the impact on optimal DC/AC ratio.



### 3. Financial calculations

#### 3.1. Revenues

Revenues were calculated for the  $5\text{MW}_P$  solar farm by multiplying the energy produced in each half-hourly settlement period by the marginal cost of energy in the same time period, and accrued over the course of the year. It was assumed there were no penalties for under or over generation. The time-resolved accrual of income over the year is shown in Figure S5 a). If conventional Silicon PV is used, a revenue of about  $194\text{k}\text{€}$  is predicted, whilst CFPVs with  $t_{TiO_2} = 48 \mu\text{m}$  CFPV, are predicted to give a revenue of  $315\text{k}\text{€}$ , and lastly a revenue of  $611\text{k}\text{€}$  is predicted for the SolarPrint CFPV. The increase in revenue for CFPV is not solely due to the increased capacity factor, as consideration must also be made for the time at which energy is generated from these technologies, and the tendency for prices during the evening and morning to be at a premium, as in illustrated in figure S5 b). We highlight that this analysis is only appropriate when the generation of renewable energy does not impact the marginal cost of energy.

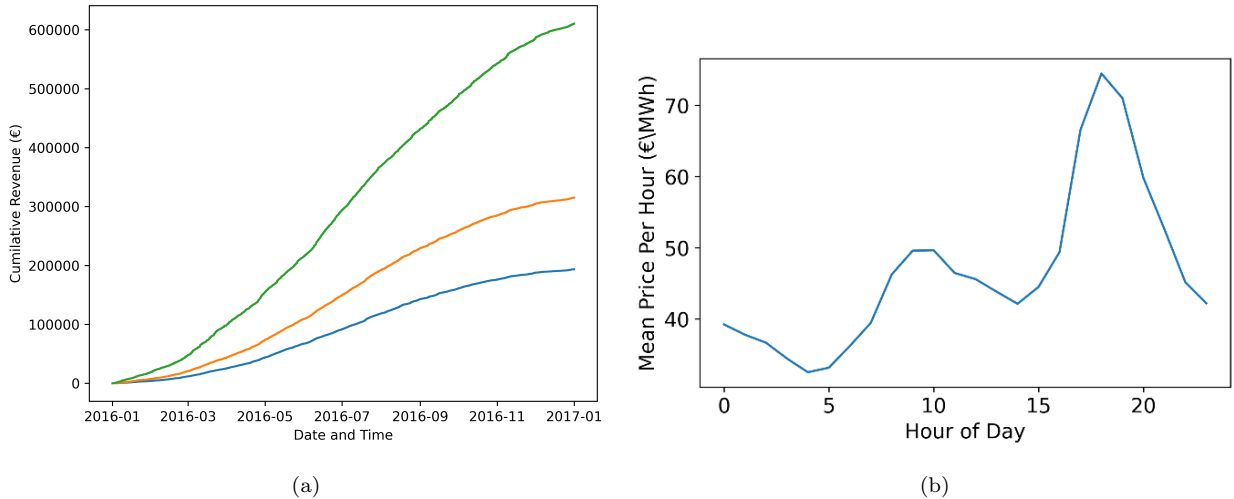


Figure S5: a) the Cumulative revenue of a silicon (blue),  $t_{TiO_2} = 48 \mu\text{m}$  CFPV (orange), and Solarprint (green)  $5\text{MW}_P$  farm selling energy to the wholesale market during 2016. b) The mean price of each settlement period in 2016.

Install costs presented in table 1 are whole project costs. The installation costs were calculated in the manner presented by Nieto-Diaz et al<sup>6</sup>. Cost of factors such as farm design,

cabling, labor and maintenance scaled with the number of panels, whilst land rent scales with the area to supply the rated capacity, allowing for appropriate spacing to avoid shading. Thus, PV devices with lower PCE attract higher land rent costs to achieve the same rated capacity of generation.

Whilst it is possible that the labour costs of Solar PV may be reduced for non-Silicon technologies, we instead assumed that the labour costs for CFPV were the same as for conventional Silicon PV. A rental model for the farm was assumed, for which the land rent per annum per m<sup>2</sup> in the UK is of the order £700 to £1000 per annum per acre or 0.17 to 0.25 £/annum m<sup>2</sup>.<sup>7,8</sup> We assumed costs at the midpoint between these two values (£0.28/annum m<sup>2</sup>) to calculate the rental cost for the first year of the project. The first year land rental cost of each presented device can be seen in table S3. Land rent, operational and maintenance costs are assumed to increase with a rate of inflation of 1.7% over the 20 year lifespan of the solar farm.

Device	Land Rent per Annum (k€)
Conventional Si PV	20.1
DS PV (Fig 1), $t_{TiO_2} = 12\mu\text{m}$	43.2
DS PV (Fig 1), $t_{TiO_2} = 18\mu\text{m}$	48.0
DS PV (Fig 1), $t_{TiO_2} = 24\mu\text{m}$	51.2
DS PV (Fig 1), $t_{TiO_2} = 48\mu\text{m}$	90.5
SolarPrint DS PV (Fig.1)	486.4

Table S3: First year land rental costs of a 5MW<sub>P</sub> Solar farm in the UK for each respective device

### 3.2. Module Cost Model

Module cost models were assessed based on the work of Bristow et al<sup>9</sup> set out in their Fig. 7. The process entailed the development of a cost model that adopted a bottom-up approach in alignment with Anderson<sup>10</sup>, where each of the individual cost elements were identified and included within the model. This approach separates costs into variable and fixed cost components. In the context of the cost categories as defined by the Association for the Advancement of Cost Estimate, AACE, International this research resides within Class 4 (Feasibility Study)<sup>11</sup>. Manufacturing plant capacity calculations are based on a facility that

can accommodate minimum BIPV production volumes of 30 MW/year. Dye-sensitised PVs are a relatively new technology with limited commercial products available in the market. The cost figures used are derived from the academic literature, bulk chemical suppliers, equipment manufacturers and private communication with RTO organisations. An Excel workbook detailing these calculations are available via the DOI link in the 'Data and Code availability' section of the main paper.

#### 4. Effect of Electrolyte Concentration on PCE-Irradiance Characteristics

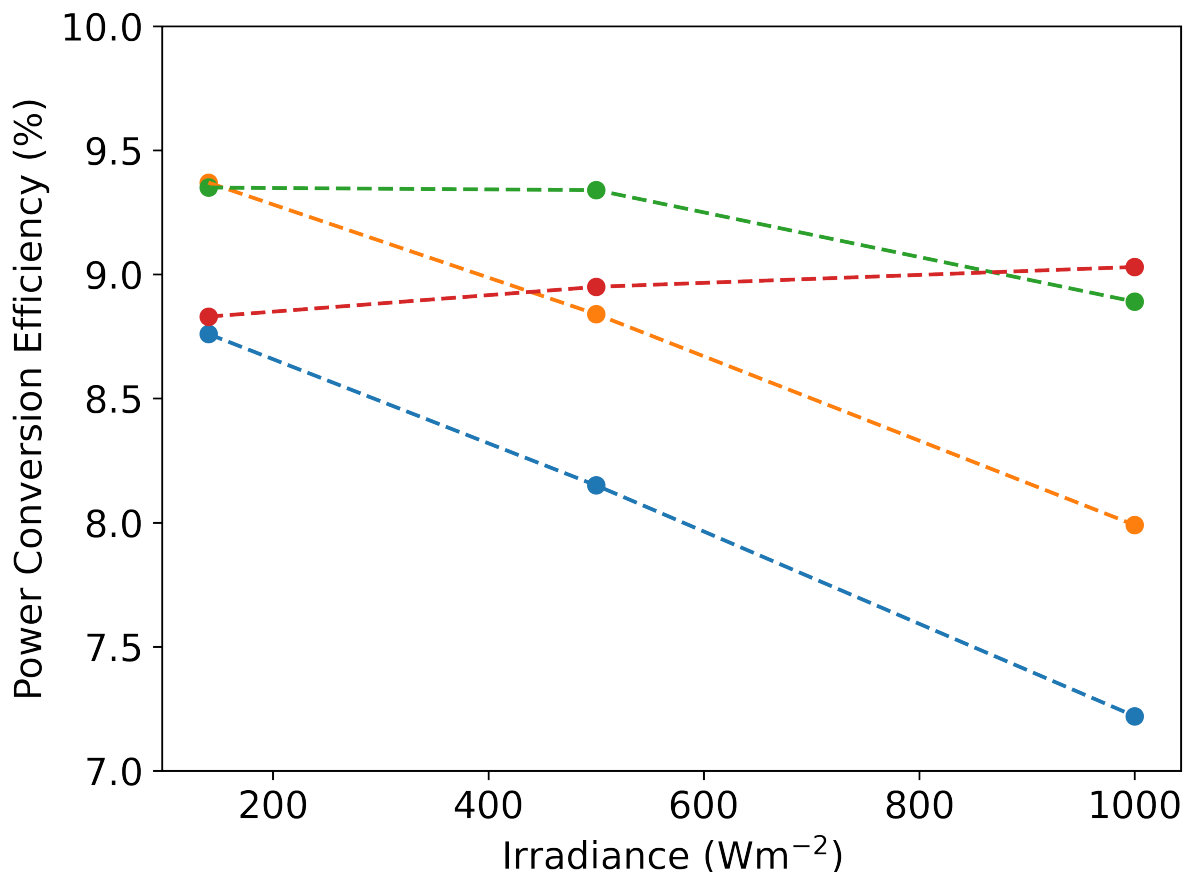


Figure S6: PCE irradiance characteristics of CFPV devices through modification of electrolyte Cu<sup>2+</sup> concentration with Cu<sub>M</sub><sup>2+</sup> = 0 M (blue), 0.01 M (orange), 0.02 M (Green) and 0.06 M (red). The concentration of Cu<sup>1+</sup> was kept constant between all devices at 0.2 M.

#### References

- [1] Andrew Crossland et al. “Assessment of electricity decarbonization scenarios for New Zealand and Great Britain using a plant dispatch and electrical energy storage modelling framework”. In: *Energies* 13.11 (2020), p. 2799.
- [2] *About Us — BMRS*. URL: <https://www.bmreports.com/bmrs/?q=help/about-us> (visited on 09/23/2022).
- [3] IPCC Climate Change et al. “Mitigation of climate change”. In: *Contribution of working group III to the fifth assessment report of the intergovernmental panel on climate change* 1454 (2014), p. 147.
- [4] *PV\_Live – Sheffield Solar*. URL: <https://www.solar.sheffield.ac.uk/pvlive/> (visited on 09/23/2022).
- [5] Global Solar Atlas. *Online* <https://globalsolaratlas.info/map>. 2023.

- [6] Balder A Nieto-Diaz, Andrew F Crossland, and Christopher Groves. “A levelized cost of energy approach to select and optimise emerging PV technologies: The relative impact of degradation, cost and initial efficiency”. In: *Applied Energy* 299 (2021), p. 117302.
- [7] *Advice for farmers on letting land for solar projects - Farmers Weekly*. URL: <https://www.fwi.co.uk/business/diversification/farm-energy/advice-for-farmers-on-letting-land-for-solar-projects> (visited on 09/23/2022).
- [8] *Renting land to solar company*. en-US. URL: <https://thefarmingforum.co.uk/index.php?threads/renting-land-to-solar-company.342601/> (visited on 09/23/2022).
- [9] Laurie Hughes et al. “Assessing the potential of steel as a substrate for building integrated photovoltaic applications”. In: *Applied energy* 229 (2018), pp. 209–223.
- [10] John Anderson. “Determining manufacturing costs”. In: *CEP* (2009), pp. 27–31.
- [11] ACCE International. “Practive No. 18-R97”. In: *Cost Estimate Classification System – As Applied in Engineering, Procurement, and Construction for the Process Industries*. Morgantown, WV: ACCE International, 1997.